SSRG International Journal of Electrical and Electronics Engineering
ISSN: 2348-8379/ https://doi.org/10.14445/23488379/IJEEE-V13I3P102

Volume 13 Issue 3, 11-22, March 2026

Original Article

Optimal Placement of Electric Vehicle Charging Stations in Electrical Radial Distribution Systems using Artificial Eagle Optimization Algorithm for Power Loss Minimization and Voltage Profile Improvement

I. Narasimha Swamy[1], P. Ravi Babu[2], A. Jaylaxmi[3]

[1,3]*EEE Department, JNTUH, Kukatpally, Hyderabad, Telangana, India.*
[2]*EEE Department, Sreenidhi Institute of Science and Technology, Hyderabad, Telangana, India.*

[1]*Corresponding Author : swamynarasimha.121@gmail.com*

Received: 05 December 2025 Revised: 04 January 2026 Accepted: 03 February 2026 Published: 31 March 2026

Abstract - *Electric Vehicles (EVs) are rapidly becoming a mainstream option for road transport, largely because they can reduce the environmental impacts associated with conventional fuel-based vehicles. However, widespread EV adoption requires a dense network of charging stations, and the resulting charging demand can stress Radial Distribution Systems (RDS) through higher losses and weaker voltage profiles if stations are sited poorly. This paper addresses the EV Charging Station (EVCS) placement problem by searching for suitable buses and station sizes on standard IEEE 33- and 69-bus networks under practical operating constraints. A novel metaheuristic, the Artificial Eagle Optimization Algorithm (AEOA), is employed for multi-objective planning, balancing loss reduction and voltage quality indicators such as VSI and AVDI. The two-stage search behaviour of AEOA supports both exploration and fine exploitation, leading to fast and stable convergence. Performance is benchmarked against well-known methods, including ALO, FPA, HBA, and TLBO. Simulation results demonstrate that the AEOA-based planning strategy consistently yields improved voltage profiles and lower power losses, thereby supporting more reliable and secure operation of RDS under increasing EV penetration.*

Keywords - *Radial Distribution Systems (RDS), Electric Vehicles (EVs), Charging Stations (CSs), Voltage Stability Index (VSI), Average Voltage Deviation Index (AVDI), and Artificial Eagle Optimization Algorithm (AEOA).*

1. Introduction

The use of fossil fuels has skyrocketed in recent years, especially in the transportation and power-generating sectors. These sources worsen environmental degradation because of their release of greenhouse gases and their role in global warming [1]. The use of fossil fuels has skyrocketed over the past few years, especially in the transportation and power-generating sectors. Many countries are aiming to transition from gasoline-powered automobiles to clean energy vehicles, such as Electric Vehicles (EVs), in an effort to reduce pollution [2]. Compared to gasoline-powered cars, electric vehicles are more economical and ecologically benign. EVs may function as regulated loads on a grid because of their advanced batteries and power electronics. The possibility of overload-associated transmission line thermal restrictions being broken, which might lead to voltage drops in certain network buses that are sensitive, is one of the main challenges to EV integration in a power system. Fast Charging Facilities (FCSs), which notably depend on grid power to reduce the amount of time required to reach the battery's State-Of-Charge (SOC) criteria. They are often used at public charging facilities to charge EVs. However, the high-power requirement of these stations has a detrimental effect on the distribution network, leading to an increase in real-power losses and voltage variations. Finding the ideal places for FCSs within the power distribution network is crucial to minimizing the negative consequences that they cause. This research offers an ideal EVCS planning strategy that supports the long-term growth of EV infrastructure through lowering real-power losses, increasing voltage stability, and enhancing overall system performance.

Using Loss Sensitivity Factor and Newton–Raphson analysis, an IEEE 33-bus system's ideal EVCS placement is examined and compared to PSO and HHO methods [3]. Several established methods have been used to identify the ideal FCS sites and sizes. Xiong et al. [4] presented a game-theoretic framework for the best fast EVCS placement. In [5], a site selection approach was developed to identify suitable charging facility locations that promote EV adoption. Erbaş et

al [6] presented a GIS-based FMDA approachology which utilizes fuzzy AHP and TOPSIS for the identification of ideal station placement. A unique EVPI approach was introduced in [7] to ensure the best EVCS placement while preserving power distribution network performance. Dong et al. [8] employed a maximum coverage position model in conjunction with a point-in-process statistical framework to enhance the effectiveness of charging facility placement. Fredriksson et al [9] studied the RNC challenge of choosing the best places for EVCS in road systems using a continuous approximation method. Additionally, a PLM plan for the best EVCS allocation was provided by [10], taking into account both EV energy loss while traveling and grid loss prevention

[11] created the MILP model, which takes into consideration both conventional and transit systems. To ascertain the best positioning and operation of Plug-in Electric Vehicle Fast Charging Stations (PEVFCSs), Hashemian et al. present an interdisciplinary approach in [12] for coordinated EVCS planning in integrated traffic–electric networks, proposing a model to optimize station siting, sizing, transportation routes, distribution networks, and recharge stations. To address the integration difficulty, [13] strategically selects the best locations for EVCS using a hybrid Genetic Algorithm and Simulated Annealing method (GA-SAA). To minimise losses and enhance performance, Chakraborty et al. [14] divide the network into three zones and use the Symbiotic Organisms Search approach to investigate the IEEE 33-bus RDS's best EVCS location.

A Grey Wolf Optimization-based strategy is presented in [15] for EVCS location in an IEEE 33-bus network that enhances bus-voltage profiles, reduces real-power losses, and shows resistance to irregular charging patterns. A Symbiotic Organisms Search algorithm [16] is presented for best EVCS–PV integration in an IEEE 69-bus RDN, seeking to raise dependability and reduce real-power losses. Optimal EVCS placement with PV integration is analysed for IEEE 33- and 69-bus systems using EP, PSO, and GWO. The present study analyses EV charging impacts on Maltese LV networks using smart metering and numerical studies, showing that feeder characteristics notably affect voltage stability and network challenges. EV charging impacts analysed in [17] on Maltese LV networks using smart metering and numerical studies show that feeder characteristics notably affect voltage stability and network challenges. For the deployment of EVCS in an IEEE 33-bus system, a Binary Random Dynamic Arithmetic Optimisation Algorithm (BRDAOA) is presented in [18], resulting in reduced losses and quicker computation, and superior reliability compared to AOA and metaheuristics. A MILP-based coordinated PDN-TN planning model is introduced in [19] for integrating EVCS placement, PDN expansion, and TN upgrades, with case studies confirming enhanced efficiency, feasibility, and user rationality in urban networks.

Recent studies emphasize that careful selection of EV charging station sites and sizes is essential for maintaining acceptable performance in distribution networks. In this work, the IEEE 33- and 69-bus radial systems are used as benchmark test beds to identify suitable buses for charging-station integration while respecting system limits. The Artificial Eagle Optimization Algorithm (AEOA) is adopted to handle the constrained, multi-objective nature of the allocation problem. Five planning scenarios are examined, and the obtained solutions are compared with several existing soft-computing and metaheuristic approaches.

2. Problem Formulation

The Voltage Stability Index (VSI) and bus-voltage profile decrease as EVCSs raise real-power losses and fluctuations in voltage with more loads. The present study examines EVCSs in RDS. To enhance system voltage functionality and reliability while reducing losses and voltage fluctuations, a multi-objective optimization is designed. A Radial Power Distribution Network's (RDS) load flow is solved using the BW/FW LF approach [20].

2.1. Multi-objective function

Here is a mathematical explanation of the suggested multi-objective optimization function.

$$\text{MOF}= \min \left(w_1 f_1 + w_2 f_2 + w_3 \left(\frac{1}{f_3}\right)\right) \quad (1)$$

Equation 2 defines the RDS's real power losses, which are based on the proposed test system's reactive and real power flow.

$$f_1 = P_{loss} = \sum_{k=1}^{nl} \frac{r_{ij}(P_j^2 + Q_j^2)}{V_i^2} \quad (2)$$

The second goal, which is expressed mathematically in Equation 3, is to lower the AVDI.

$$f_2 = AVDI = \frac{1}{NB} \sum_{I=1}^{NB} |1 - V_i| \quad (3)$$

Enhancing the VSI of the suggested test system is the third goal, which is described as

$$f_3 = VSI_j = [|V_i|^4 - 4\left(P_j x_{ij} - Q_j r_{ij}\right) - 4(P_j r_{ij} + Q_j x_{ij})|V_i|^2] \quad (4)$$

Equation 4 states the presented multi-optimization objective, which is reduced while taking into account operational restrictions on branch Power Flows (|Si|) and Node Voltages (Vi), as well as design restrictions on Charging Facilities (CSs), such as the Quantity Of Charging Facilities (CSs) and Charging Points (CPs), as specified in Equations 5 to 8.

Voltage limit constraints

$$V_{min} \le V_i \le V_{max} \quad \text{i=1,2,…nb} \tag{5}$$

Total power limit constraints

$$|S_l| \le |S_{l,max}| \quad \text{i=1,2,…nbl} \tag{6}$$

Charging point limit constraints

$$\text{nC}P_{min} \le nCP \le nCP_{max} \tag{7}$$

Charging stations limit constraints

$$\text{nC}S_{min} \le nCS \le nCS_{max} \tag{8}$$

3. Solution Methodology

To address challenging engineering optimisation tasks, this section introduces the Artificial Eagle Optimisation (AEO) concept and explains how it motivates the Artificial Eagle Optimization Algorithm (AEOA) used in this study.

The analogy is drawn from the way trained eagles can observe, coordinate, and adjust their movement strategies to achieve a target efficiently. Translating this behaviour into computation, AEOA maintains a population of candidate solutions and updates them through two complementary phases: a broad search phase that diversifies exploration of the solution space and a refinement phase that intensifies exploitation near promising regions.

This balance helps avoid premature convergence and improves solution quality for non-linear, constrained problems such as optimal EVCS allocation in distribution networks.

3.1. The Population Initialization Stage

Equation 9 shows how a dim decision variable single objective minimization issue is often formulated.

$$min\, f\,(X^*) = f([x_1^*, x_2^*, \ldots, x_{dim}^* \tag{9}$$

$$s.t. x_i^{min_{ii}^{*max}},$$

Where the fitness value for the present candidate solution is denoted by $f(X^*)$, and $X^* = [x_1^*, x_2^*, \ldots, x_{dim}^*$ represents one possible way to solve the optimization challenge. A solution with great precision is indicated by a smaller fitness value.

$Lb = [x_1^{min_2^{min_{dim}^{min]}}}$ Moreover, $ub = [x_1^{max_2^{max_{dim}^{max]}}}$ are the upper and lower limits that variables must meet. N potential solutions with the following formulation are created at random by the AEOA for the inaugural artificial eagle population.

$$Pop = \begin{bmatrix} Pos_1 \\ Pos_2 \\ . \\ . \\ . \\ Pos_N \end{bmatrix} = \begin{bmatrix} X_{1,1}\ X_{1,2} \ldots X_{1,dim} \\ X_{2,1}\ X_{2,2} \ldots X_{2,dim} \\ \vdots\ \ \vdots\ \ \ddots\ \ \vdots \\ X_{N,1}\ X_{N,2} \ldots X_{N,dim} \end{bmatrix} \tag{10}$$

Here, Posi denotes Equation (11), which is used to calculate the artificial eagle's position, which corresponds to candidate solution X∗ in Equation (9).

$$Pos_i = Lb + rand.(ub - Lb), 1 \le i \le N. \tag{11}$$

Where the random integer "rand" ranges from 0 to 1.

3.2. Situational Awareness and Analysis Stage

Artificial eagles enhance their intelligence through manual intervention, especially during migration, where they assess the population's state. Each eagle updates its position using better-positioned peers. Positions are ranked by fitness, and an eagle's position depends on the three best ones: Posγ, Posβ, and Posα (β,α, γ ≠ i).

Equation (5) will then produce a possibly more appropriate position.

$$NewPos_i(t) = (Pos_\alpha(t) \pm s.(Pos_\beta(t) \pm Pos_\gamma(t)) \tag{12}$$

The attenuation coefficient is given by S=1.2−t/T, which lowers as the iterations progress. Here, t is the current iteration, and T is the maximum number of iterations. In the early phase (small t), a larger S allows broader exploration of the solution space, helping the algorithm move closer to the best solution. In the later phase (large t), a smaller S preserves population quality. The stochastic character of the process is shown by the randomly selected signs that are positive and negative in Equation 12. To represent the unpredictability of the thought process, Equation 12 is chosen at random.

Equation 13 illustrates how the artificial eagle uses the greedy selection approach to find better positions following consideration and analysis.

$$\begin{cases} Po\ _i(t+1)=Pos_i(t), & if \quad f(po\ _i(t)) < f(NewP\ \ _i(t)), \\ Po\ _i(t+1)=NewPos_i(t), & if \quad f(pos_i(t)) \ge f(NewPos_i(t))_i, \end{cases} \tag{13}$$

For New Posi(t) and $Pos_i(t)$, respectively, the fitness values are denoted by f (New $Pos_i(t)$) and f ($Pos_i(t)$).

3.3. Free Exploration Stage

The most common location and a random length of step or direction determined by environmental input may be used to transfer it to a new candidate location. Every artificial eagle may independently update its position while migrating. This

behavior demonstrates strong exploration ability in complex decision spaces. To model this stage, two modes are defined.

In the first mode, shown in Equation 14, eagles use a Levy flying pattern to circle the ideal location.

$$Pos_i(t+1) = Pos_i(t) + levy.(Pos_{best}(t) - Pos_i(t)) \quad (14)$$

where $Pos_{best}(t)$ is the optimal site closest to the levy and migratory destination, and where the artificial eagle with the smallest fitness value is located. It is a random value that follows the Levy distribution. This approach is overly dependent on the optimal position at the moment.

Local optima may cause the accuracy of the solution to decrease if that position represents local conditions. Equation 15 illustrates how a more haphazard approach is employed to get around this.

$$Pos_i(t+1) = (Pos_p(t) - rand.Pos_{ave}(t)) \quad (15)$$

Where $Pos_{ave}(t) = (Pos_{r1}(t) + (Pos_{r2}(t) + (Pos_{r3}(t))/3$ is the mean of three positions chosen at random. $(Pos_p(t)$ is acquired by merging the ideal position, which is done in this way:

$$Pos_p(t) = (1-\beta).Pos_{ave}(t) + \beta.Pos_{best}(t) \quad (16)$$

where β ranges from 0 to 1. The algorithm will execute the two aforementioned modes with equal probability, as indicated by Equation 17.

$$\begin{cases} Pos_i(t+1) = Pos_{best}(t).levy + Pos_i(t), & if \quad rand > 0.5, \\ Pos_i(t+1) = (Pos_p(t) - rand.Pos_{ave}(t)), & if \quad rand \leq 0.5. \end{cases} \quad (17)$$

3.4. Flight Formation Integration Stage

Consequently, the flight formation integration behavior is represented by a novel formation flying method based on distance data. Because they are trained by hand, artificial eagles are also aware of collaboration while they are walking freely. To begin, a distance vector must be computed to document the separation between a point and other positions. By sorting distances from smallest to largest, an ordered distance vector is formed. The artificial eagle updates its position by targeting a farther location.

Figures 1 and 2 illustrate this pattern: in Figure 1, eagles choose nearby targets and form small groups, while in Figure 2, they move farther away, guaranteeing stability in the search by effectively ensuring that everyone moves in unison to more suitable locations. Equation 18 illustrates how the fake eagle will revise its location after identifying the target ith.

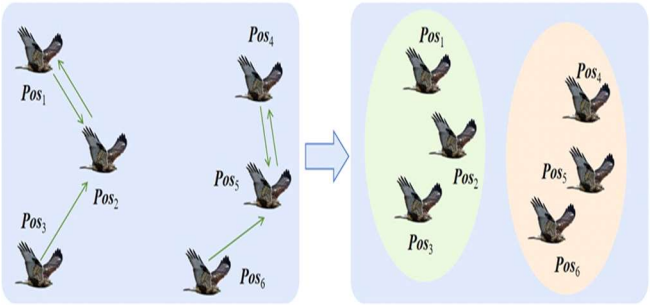

Fig. 1 Pattern of position updates based on the closest distance

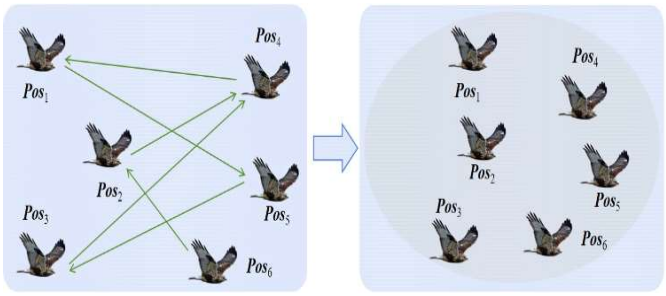

Fig. 2 Pattern of position updates based on the far distance

$$\begin{cases} Po_i(t+1) = Pos_i(t) + R.(Target_i - I.Pos_i(t)), & if \quad f(target_i) > f(Target_i) < f(Pos_i(t)), \\ Po_i(t+1) = Pos_i(t) + R.(Pos_i(t) - Target_i), & if \quad f(target_i) \geq f(Target_i) < f(Pos_i(t)), \end{cases} \quad (18)$$

Where the random components in the vector R range from 0 to 1.

3.5. AEOA Approach Implementation for the Problem of Optimal EVCS Allocation

1. Read the network data (IEEE-33 or IEEE-69 bus system), including bus coordinates, load data, branch impedances, EVCS candidate buses, EVCS ratings or maximum EV loads, and system constraints.
2. It is necessary to set the population size (N) and the maximum number of iterations (T).
3. Initialize the population of eagle positions, where each individual represents a specific EVCS placement and size configuration.
4. Analyze the forward-backward sweep load flow and assess the objectives.
5. Update the global best and personal best positions.
6. Generate new candidate positions and move toward better solutions.
7. Check rand ≥ 0.5to update the position.
8. Select target solutions based on their distance (fitness value) and update the positions toward these targets.
9. Analyze the forward–backward sweep load flow for the newly generated positions to evaluate their fitness.
10. Check iteration count, t ≤ T, if YES, move back to step 6, if NO, stop the iteration and perform the final forward–backward sweep load flow and compute objective(s) and compare with base case.

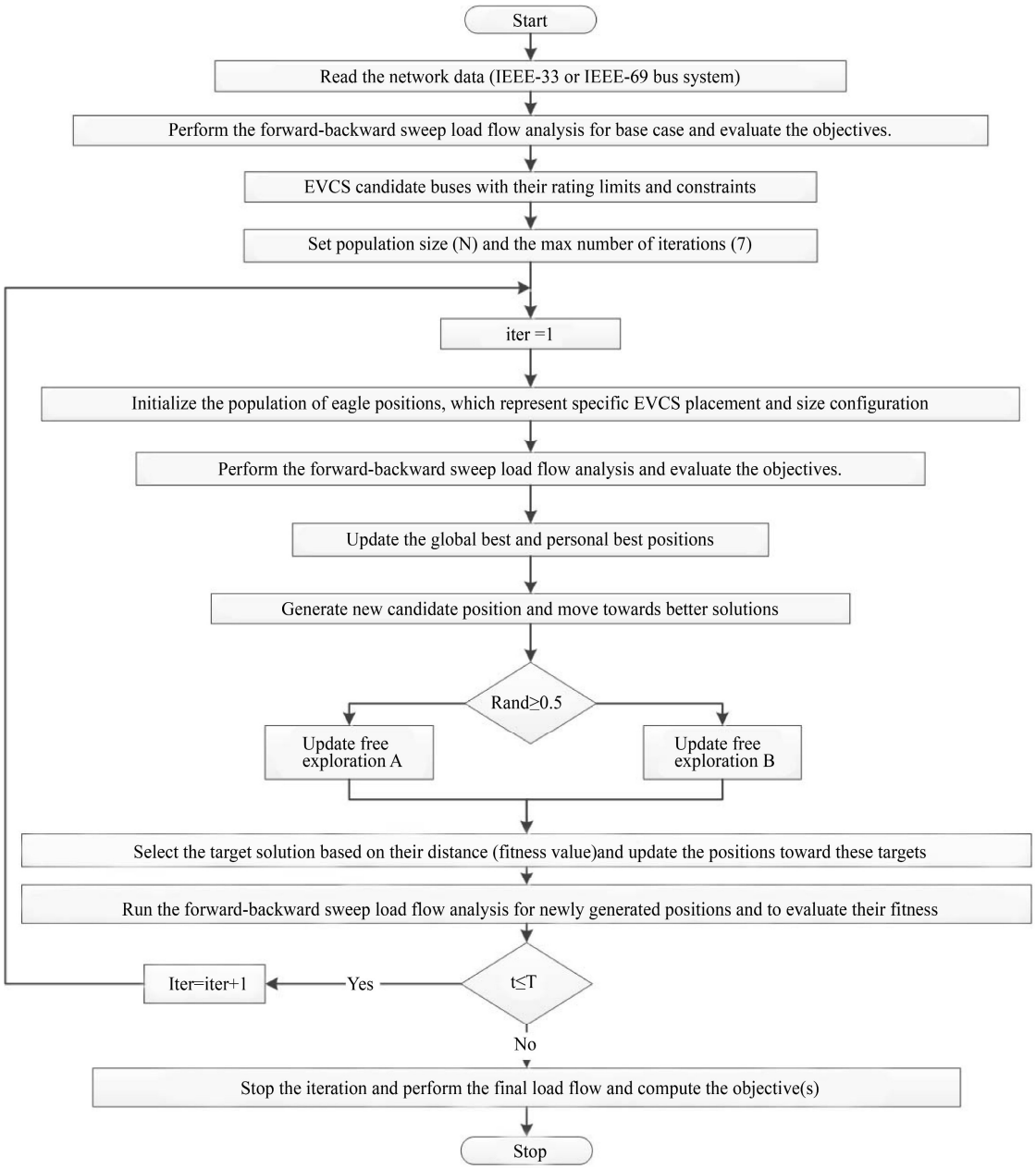

Fig. 3 The Flow Chart of the AEOA

Figure 3 illustrates the entire AEOA flow chart for implementation and reference based on the aforementioned steps.

4. Results and Discussion

Bus and line data from [22] are used to test the proposed AEOA on the standard IEEE 33- and 69-bus network. Battery Electric Vehicles (BEVs) and Plug-In Hybrid Electric Vehicles (PHEVs) are both taken into consideration, and each has a designated Charging Port (CP). Design parameters, including EV types, CP count, power ratings, and total station capacity, are adopted from [24], where charging station power ratings range from 975 to 1674.5 kW.

4.1. Test System 1: 33-Node Test System

Data from [23] was used to test the proposed AEOA on the IEEE 33-bus network. With loads of 3715 kW and 2300 kVAr, the system runs at 12.66 kV. 7 variables, 100 iterations, and a population size of 40 were the AEOA settings.

The system is evaluated in five scenarios: Case 1 – base load flow; Case 2 – increased load with minimum CPs at lowest power; Case 3 – high load with maximum CPs at full power; Case 4 – optimal EVCS placement via AEOA with minimum CPs/power; Case 5 – optimal placement via AEOA with maximum CPs/power.

In Case 1, the allocation of load flow is evaluated to ascertain the voltage deviation index, optimum voltage, VSI, base-case bus voltages, and network power loss. In Case 2, 3 Charging Stations (CSs) with a minimum rating of 975 kW each were connected to each sub-feeder, raising the total load to 6640 kW (≈1.787× base load). The findings of load flow (Table 1) indicate a 576.17 kW power loss, a VSI of 0.4984 p.u., at least bus voltage of 0.8408 p.u., and an AVDI of 0.0108. The total load increases to 8738.5 kW (≈2.35× base load) in Case 3, which takes into account the most CPs at the highest CS rating of 1674.5 kW. With a 1024.39 kW power loss, a VSI of 0.3854 p.u., an AVDI of 0.0187, and a Vmin of 0.7888 p.u., the system is under more stress, suggesting that increasing load demand dramatically raises power losses and voltage variations. In order to ascertain the best location for charging stations, the suggested AEOA was applied to Cases 2 and 3, producing Cases 4 and 5. With a total load of 6640 kW for Case 4, the AEOA determined that buses 2, 26, and 49 would be the best places to install charging stations with the fewest number of CPs. By lowering the AVDI to 0.004498 p.u., improving the VSI to 0.6711 p.u., lowering the power loss to 273.82 kW, and raising the minimal bus voltage (Vmin) to 0.9051 p.u., this improvement greatly enhanced system efficiency. When compared to the base situation, Figures 4 and 5 show the enhancements in the voltage profile and VSI. From Case 2 to the optimal placement, the power loss was reduced by 52.47% overall. Table 1 shows simulation outcomes for the 33 bus system.

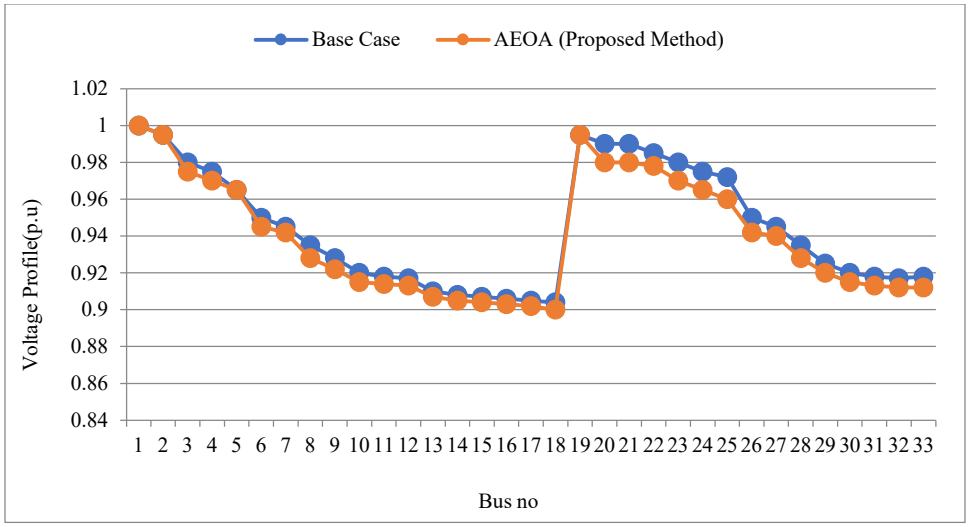

Fig. 4 Voltage profile of 33 bus system

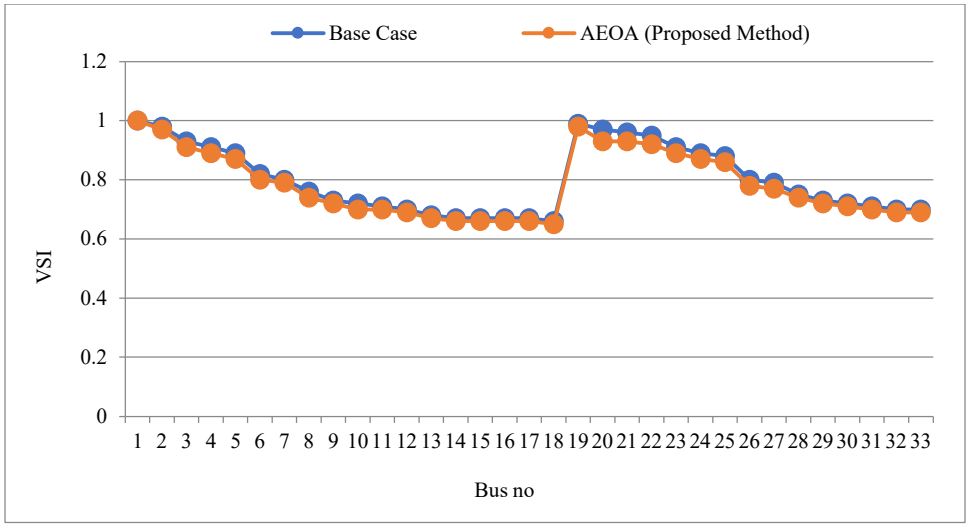

Fig. 5 VSI of 33 bus system

The AEOA was used for distribution load flow evaluation in Case 5, where the maximum number of CPs was taken into account, which gave a total system load of 8738.5 kW. Buses 2, 22, and 26 were chosen by the algorithm to be the best places for charging stations. Power loss dropped to 378.15 kW, AVDI was 0.004896 p.u., Minimum Bus Voltage (Vmin)

was 0.9049 p.u., and VSI was 0.6524 p.u., all of which indicated a significant improvement in system performance. The success of the proposed technique was demonstrated by the 63.08% reduction in power loss when compared to Case 3 without optimization.

The IEEE 33-bus system's convergence parameters are shown in Figure 6. Furthermore, simulation outcomes were contrasted to the HBA and TLBO techniques; the improvements of the AEOA are displayed in Table 1 and Figures 7 to 9.

Table 1. Simulation outcomes for the 33 bus system

Cases and load	Methods	Locations of EV Charging Stations	VSI (p.u)	Power losses (KW)	AVDI (p.u)
Case 1 (Base Case) 3715 kW	--	--	0.667174	210.9897	0.0040541
Case 2 6640 kW	--	--	0.4984	576.1705	0.0108
Case 3 8738.5 kW	--	--	0.3854	1024.3908	0.0187
Case 4	AEOA (proposed)	2, 22, 26	0.6711	273.82	0.004498
	FPA [25]	2, 19, 25	0.6499	295.6474	0.0047
	ALO [25]	2, 19, 25	0.6499	295.6474	0.0047
	TLBO [25]	2, 19, 25	0.6499	295.6474	0.0047
	HBA [24]	2, 20, 23	0.651445	281.29	0.0046898
Case 5	AEOA (proposed)	2, 22, 26	0.6524	378.1462	0.004896
	FPA [25]	2, 19, 25	0.6381	390.6266	0.0053
	ALO [25]	2, 19, 25	0.6381	390.6266	0.0053
	TLBO [25]	2, 19, 25	0.6381	390.6266	0.0053
	HBA [24]	2, 20, 23	0.6411	384.5842	0.005121
AEOA objective function (proposed)				0.81064	

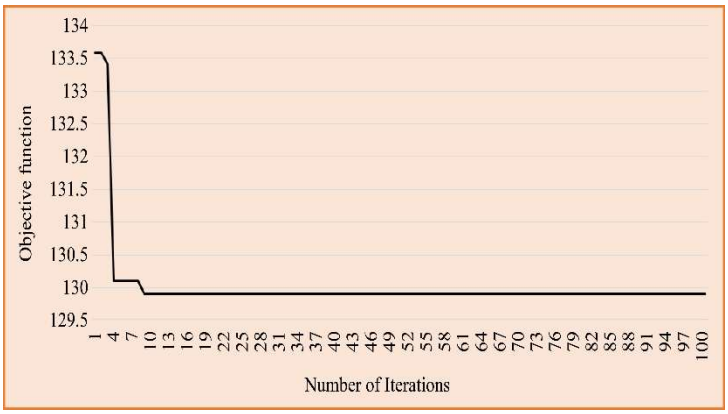

Fig. 6 Convergence curve for 33 bus system

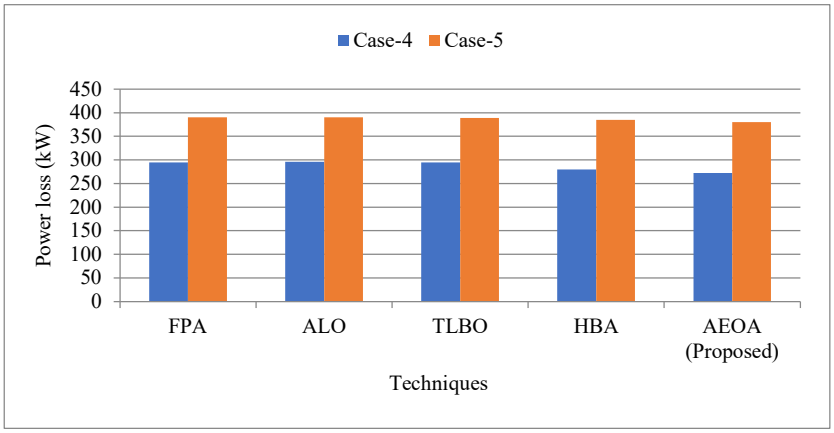

Fig. 7 Comparison of the power loss of AEOA

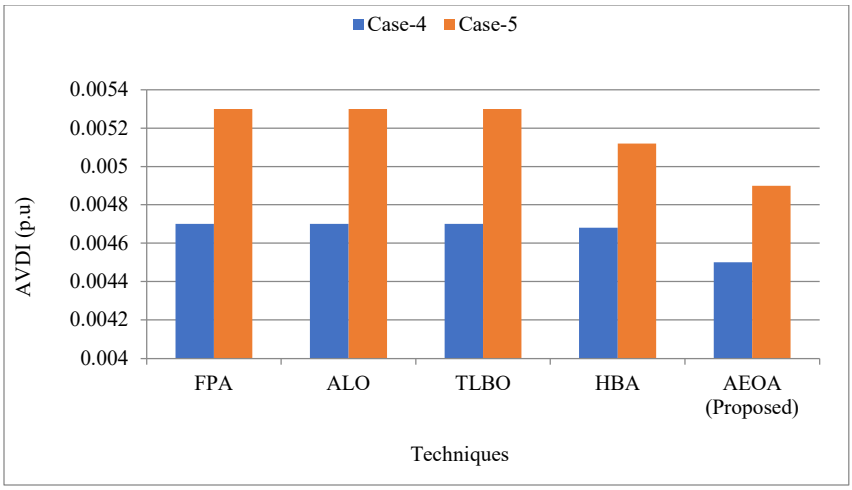

Fig. 8 Comparison of AVDI of AEOA with TLBO and HBA

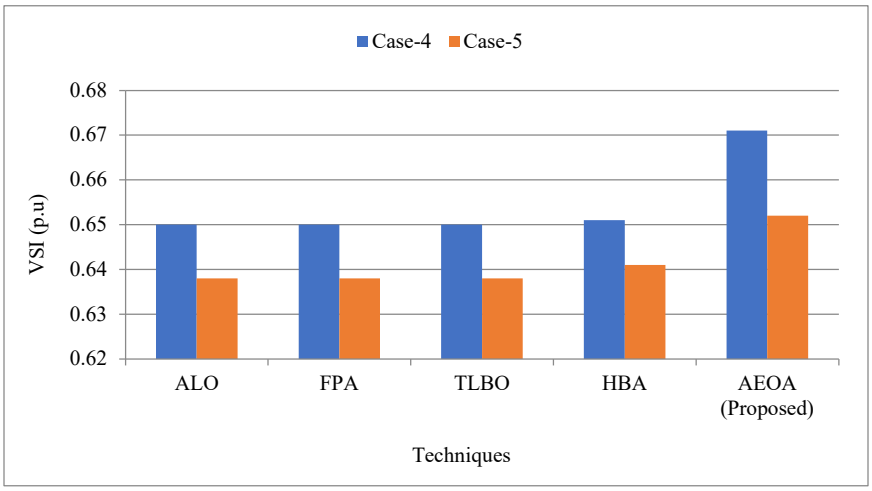

Fig. 9 Comparison of VSI of AEOA with TLBO and HBA

4.2. Test System 2: 69-Node Test System

Data from [23] was used to test the proposed AEOA on the IEEE 69-bus network. With loads of 3801.4 kW and 2693.6 kVAr, the system runs at 12.66 kV. 7 variables, 200 iterations, and a population size of 50 were the AEOA settings.

The proposed system is evaluated under five test scenarios. Case 1 considers the base distribution load flow. Increased demand is imposed by Case 2 with the minimum CPs at the lowest CS grade, while Case 3 considers maximum demand with the highest number of CPs at full CS rating. Case-4 determines optimal EVCS placement using the AEOA with minimum CPs, and Case-5 evaluates optimal placement with maximum CPs at the highest rating.

Distribution load flow studies are used in Case 1 to assess power loss and minimum voltage. VSI, bus voltages, and AVDI. In Case-2, three EV-CSs (one per sub-feeder) with minimum CPs impose a total demand of 2925 kW, raising the system load to 6726.4 kW (1.7695 times Case-1) from 3801.4 kW. As a result, real losses rise from 224.8807 kW to 613.4994 kW (72.81% higher), VSI decreases from 0.6823 to 0.5114, AVDI rises from 0.0014 to 0.004, and the minimum voltage falls from 0.9092 p.u. to 0.8462 p.u.

In Case 3, the system loading increases from 3801.4 kW to 8824.9 kW at a total EVCS demand of 5023.5 kW with three CSs (maximum CPs), i.e., 2.3215 times that of Case 1. Consequently, real losses increase from 224.8807 kW to 1108.6 kW (292.97% higher than Case-1 and 172.81% higher than Case-2), and AVDI increases from 0.0014 to 0.0072. The minimum voltage at bus-65 decreases from 0.9092 p.u. to 0.7935 p.u., while the VSI decreases from 0.6823 to 0.3949.

The proposed AEOA, applied in Cases 2 and 3, determines the optimal CS allocation, represented as Cases 4 and 5. In Case 4, with an overall load requirement of 6726.4 kW, the AEOA identifies buses 2, 26, and 49 as optimal locations having the least amount of CPs. Compared to the base case, losses reduce from 613.4994 kW to 225.1025 kW, AVDI decreases from 0.004 to 0.001381, and VSI improves from 0.5114 to 0.691201. The minimum voltage also increases

from 0.8462 p.u. to 0.9095 p.u. The VSI and voltage profiles for the base case and Case 4 are shown in Figures 10 and 11. In Case-5, the AEOA identifies buses 2, 26, and 49 as optimal CS locations, reducing system losses from 1108.6266 kW to 225.1244 kW, AVDI from 0.0072 to 0.001394, and improving VSI from 0.3949 to 0.695151. The minimum voltage also improves from 0.7935 p.u. to 0.9093 p.u. Outcomes for all cases are summarized in Table 2. Compared to Cases 2 and 3, power losses in Cases 4 and 5 (225.1025 kW and 225.1244 kW, respectively) are significantly minimized. The convergence of the 69-bus system is shown in Figure 12. Comparison of the power loss of AEOA with existing methods is depicted in Figure 13. Benchmarking against HBA, TLBO, ALO, and FPA (Table 2) confirms that the proposed CHBA method achieves superior lowering of power loss and AVDI, while enhancing voltage profile and VSI.

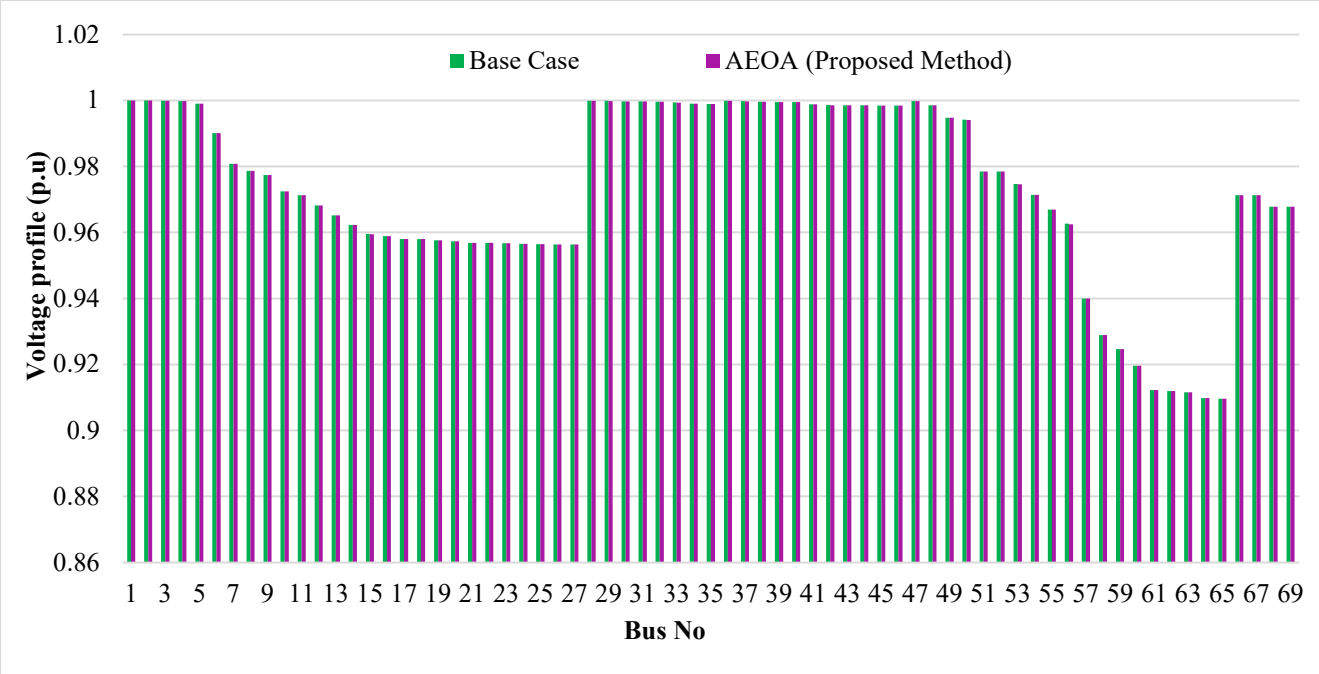

Fig. 10 Voltage profile of 69-Bus system

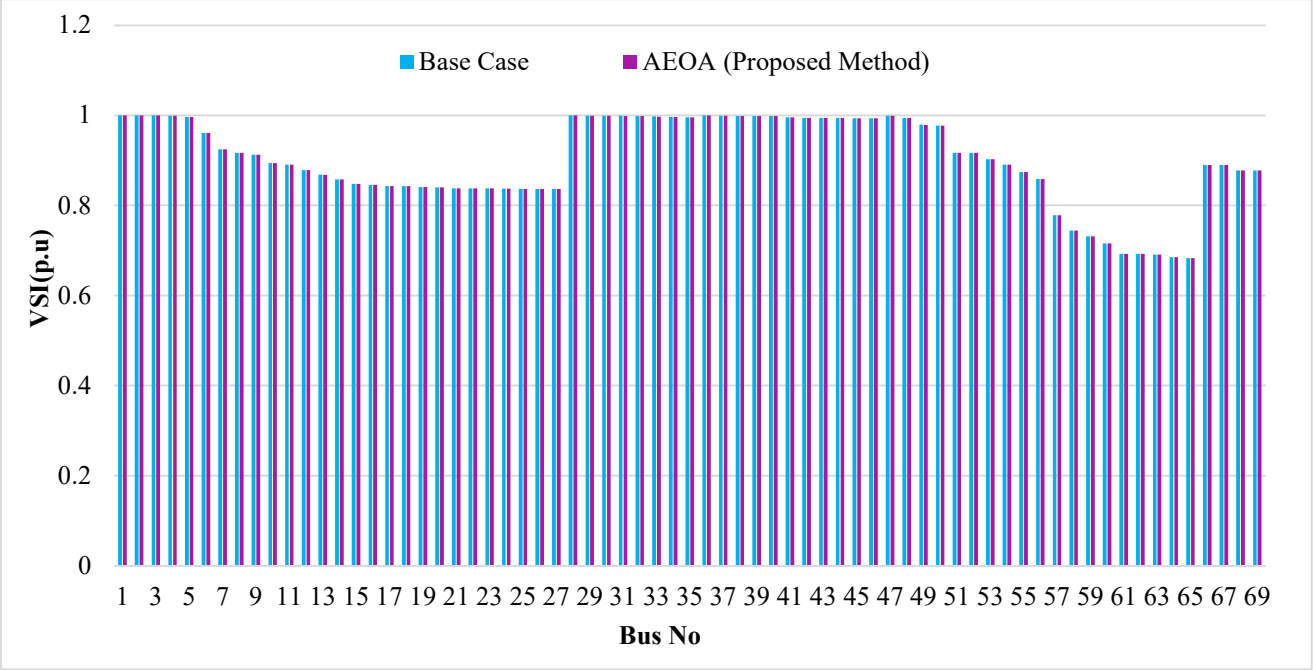

Fig. 11 VSI of 69-Bus system

Table 2. Simulation outcomes for the 69 bus system

Case	Techniques	Locations of EV Charging Stations	Power losses (KW)	AVDI (p.u)	VSI (p.u)	Vmin
Case 1(Base Case) Load 38014 kW	-		224.97	0.0014393	0.683323	0.9092
Case 2 (Load 6726.4 kW)	-		613.4994	0.004	0.5114	0.8462
Case 3 (Load 8824.9 kW)			1108.6266	0.0072	0.3949	0.7935
Case 4	AEOA (proposed)	2, 26, 49	225.1025	0.001381	0.691201	0.9095
	HBA [24]	2, 28, 3	225.1700	0.0014402	0.683274	0.9092
	TLBO [25]	2, 28, 47	225.2186	0.0014	0.6822	0.9092
	ALO [25]	2, 28, 47	225.2186	0.0014	0.6822	0.9092
	FPA [25]	2, 28, 47	225.2186	0.0014	0.6822	0.9092
Case 5	AEOA (proposed)	2, 26, 49	225.1244	0.001394	0.695151	0.9093
	HBA [24]	2, 28, 3	225.4122	0.0014493	0.683052	0.9092
	TLBO [25]	2, 28, 47	225.5766	0.0014	0.6821	0.9092
	ALO [25]	2, 28, 47	225.5766	0.0014	0.6821	0.9092
	FPA [25]	2, 28, 47	225.5766	0.0014	0.6821	0.9092

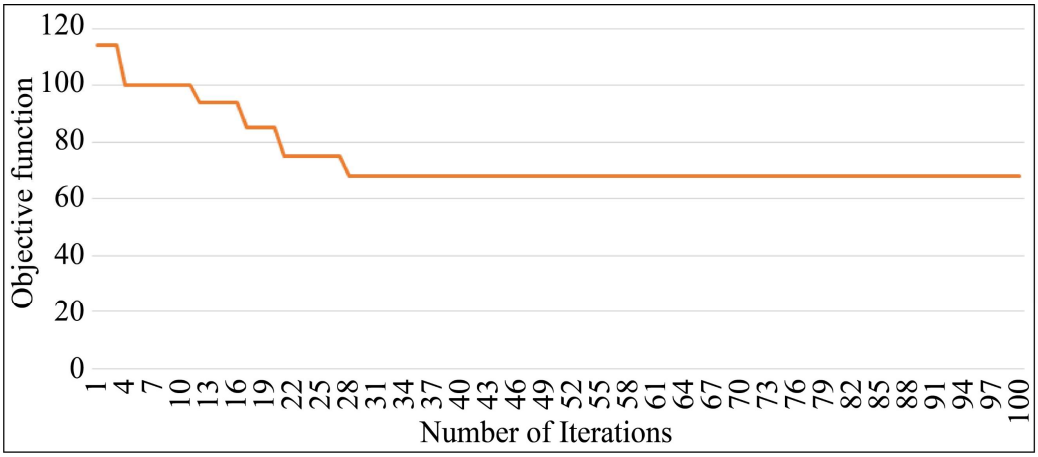

Fig. 12 Convergence curve for 69-node test system

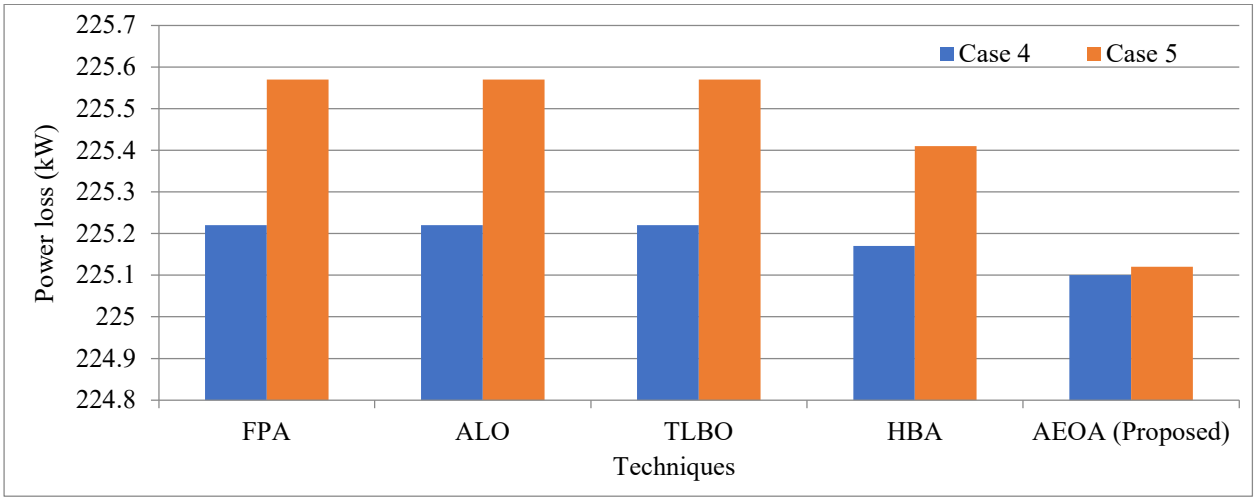

Fig. 13 Comparison of the power loss of AEOA with existing methods

5. Conclusion

An innovative stochastic search strategy called the Artificial Eagle Optimization Algorithm (AEOA) has been put forth to identify the best location for EVCSs in RDS. Exploration and exploitation are the two main search phases that AEOA uses to find the best answers quickly and with little computational effort.

The IEEE 33-bus and 69-bus case studies, in which AEOA successfully identifies the best EVCS locations and greatly enhances system performance, have verified its efficiency. Higher VSI, lower AVDI, better voltage profiles, and lower power losses are all shown by the results. When compared to well-known optimization techniques like ALO, FPA, HBA, and TLBO, AEOA exhibits better convergence speed and increased reliability. These findings confirm that AEOA is a robust and highly efficient optimization approach for complex engineering tasks like EVCS allocation in power distribution networks. Furthermore, integrating Distributed Generation (DG) with the existing system is identified as a promising direction for future work to enhance overall system performance further.

References

[1] Farivar Fazelpour et al., "Intelligent Optimization to Integrate a Plug-in Hybrid Electric Vehicle Smart Parking Lot with Renewable Energy Resources and Enhance Grid Characteristics," *Energy Conversion and Management*, vol. 77, pp. 250-261, 2014. [CrossRef] [Google Scholar] [Publisher Link]

[2] M. Hadi Amini et al., "Effect of Electric Vehicle Parking Lots' Charging Demand as Dispatchable Loads on Power Systems Loss," *2016 IEEE International Conference on Electro Information Technology (EIT)*, Grand Forks, ND, USA, pp. 0499-0503, 2016. [CrossRef] [Google Scholar] [Publisher Link]

[3] Naresh Kumar Golla, Suresh Kumar Sudabattula, and Velamuri Suresh, "Optimal Placement of Electric Vehicle Charging Station in Distribution System using Meta-Heuristic Techniques," *Mathematical Modelling of Engineering Problems*, vol. 9, no. 1, pp. 60-66, 2022. [CrossRef] [Google Scholar] [Publisher Link]

[4] Yanhai Xiong et al., "Optimal Electric Vehicle Fast Charging Station Placement based on Game Theoretical Framework," *IEEE Transactions on Intelligent Transportation Systems*, vol. 19, no. 8, pp. 2493-2504, 2018. [CrossRef] [Google Scholar] [Publisher Link]

[5] Jiwon Lee et al., "Optimal Allocation for Electric Vehicle Charging Stations," *Energies*, vol. 14, no. 18, pp. 1-9, 2021. [CrossRef] [Google Scholar] [Publisher Link]

[6] Mehmet Erbaş et al., "Optimal Siting of Electric Vehicle Charging Stations: A GIS-based Fuzzy Multi-Criteria Decision Analysis," *Energy*, vol. 163, pp.1017-1031, 2018. [CrossRef] [Google Scholar] [Publisher Link]

[7] A.N. Archana, and T. Rajeev, "A Novel Reliability Index based Approach for EV Charging Station Allocation in Distribution System," *IEEE Transactions on Industry Applications*, vol. 57, no. 6, pp. 6385-6394, 2021. [CrossRef] [Google Scholar] [Publisher Link]

[8] Guanpeng Dong et al., "Electric Vehicle Charging Point Placement Optimisation by Exploiting Spatial Statistics and Maximal Coverage Location Models," *Transportation Research Part D: Transport and Environment*, vol. 67, pp. 77-88, 2019. [CrossRef] [Google Scholar] [Publisher Link]

[9] Henrik Fredriksson, Mattias Dahl, and Johan Holmgren, "Optimal Placement of Charging Stations for Electric Vehicles in Large-Scale Transportation Networks," *Procedia Computer Science*, vol. 160, pp. 77-84, 2019. [CrossRef] [Google Scholar] [Publisher Link]

[10] Arindam Sadhukhan, Md Samar Ahmad, and S. Sivasubramani, "Optimal Allocation of EV Charging Stations in a Radial Distribution Network Using Probabilistic Load Modeling," *IEEE Transactions on Intelligent Transportation Systems*, vol. 23, no. 8, pp. 11376-11385, 2022. [CrossRef] [Google Scholar] [Publisher Link]

[11] Seyed Nasrollah Hashemian, Mohammad Amin Latify, and G. Reza Yousefi, "PEV Fast-Charging Station Sizing and Placement in Coupled Transportation-Distribution Networks Considering Power Line Conditioning Capability," *IEEE Transactions on Smart Grid*, vol. 11, no. 6, pp. 4773-4783, 2020. [CrossRef] [Google Scholar] [Publisher Link]

[12] Xu Wang et al., "Coordinated Planning Strategy for Electric Vehicle Charging Stations and Coupled Traffic-Electric Networks," *IEEE Transactions on Power Systems*, vol. 34, no. 1, pp. 268-279, 2019. [CrossRef] [Google Scholar] [Publisher Link]

[13] Boya Anil Kumar et al., "Hybrid Genetic Algorithm-Simulated Annealing based Electric Vehicle Charging Station Placement for Optimizing Distribution Network Resilience," *Scientific Reports*, vol. 14, no. 1, pp. 1-28, 2024. [CrossRef] [Google Scholar] [Publisher Link]

[14] Raj Chakraborty, Diptanu Das, and Priyanath Das, "Optimal Placement of Electric Vehicle Charging Station with V2G Provision using Symbiotic Organisms Search Algorithm," *2022 IEEE International Students' Conference on Electrical, Electronics and Computer Science (SCEECS)*, BHOPAL, India, pp. 1-6, 2022. [CrossRef] [Google Scholar] [Publisher Link]

[15] Sainadh Singh Kshatri et al., "An Enhanced Distribution System Performance with Optimization Techniques for Location of Electrical Vehicle Charging Stations," *ITEGAM-JETIA*, vol. 11, no. 54, pp. 53-59, 2025. [CrossRef] [Google Scholar] [Publisher Link]

[16] Raj Chakraborty et al., "A Strategic Approach to the Placement of PV-Integrated EV Charging Stations for Enhancing the Distribution Network Performance," *Energy Exploration and Exploitation*, vol. 43, no. 5, pp. 2015-2040, 2025. [CrossRef] [Google Scholar] [Publisher Link]

[17] Brian Azzopardi, and Yesbol Gabdullin, "Impacts of Electric Vehicles Charging in Low-Voltage Distribution Networks: A Case Study in Malta," *Energies*, vol. 17, no. 2, pp. 1-18, 2024. [CrossRef] [Google Scholar] [Publisher Link]

[18] Georgios Fotis, "An Improved Arithmetic Method for Determining the Optimum Placement and Size of EV Charging Stations," *Computers and Electrical Engineering*, vol. 120, pp. 1-16, 2024. [CrossRef] [Google Scholar] [Publisher Link]

[19] Ke Li et al., "A MILP Method for Optimal Planning of Electric Vehicle Charging Stations in Coordinated Urban Power and Transportation Networks," *IEEE Transactions on Power Systems*, vol. 38, no. 6, pp. 5406-5419, 2023. [CrossRef] [Google Scholar] [Publisher Link]

[20] Jen-Hao Teng, "A Direct Approach for Distribution System Load Flow Solutions," *IEEE Transactions on Power Delivery*, vol. 18, no. 3, pp. 882-887, 2003. [CrossRef] [Google Scholar] [Publisher Link]

[21] Shuhan Hu et al., "A Novel Artificial Eagle-Inspired Optimization Algorithm for Trade Hub Location and Allocation Method," *Biomimetics*, vol. 10, no. 8, pp. 1-27, 2025. [CrossRef] [Google Scholar] [Publisher Link]

[22] Lijun Liu et al., "Multi-Objective Coordinated Optimal Allocation of DG and EVCSs based on the V2G Mode," *Processes*, vol. 9, no. 1, pp. 1-18, 2020. [CrossRef] [Google Scholar] [Publisher Link]

[23] Sanchari Deb et al., "A Hybrid Multi-Objective Chicken Swarm Optimization and Teaching Learning based Algorithm for Charging Station Placement Problem," *IEEE Access*, vol. 8, pp. 92573-92590, 2020. [CrossRef] [Google Scholar] [Publisher Link]

[24] Madhubabu Thiruveedula, K. Asokan, and J.B.V. Subrahmanyam, "An Effective Honey Badger Algorithm based Multi-Objective Optimal Allocation of Electric Vehicle Charging Stations in Radial Distribution Systems," *Indian Journal of Science and Technology*, vol. 17, no. 13, pp. 1357-1367, 2024. [CrossRef] [Google Scholar] [Publisher Link]

[25] Ponnam Venkata K. Babu, and K. Swarnasri, "Multi-Objective Optimal Allocation of Electric Vehicle Charging Stations in Radial Distribution System using Teaching Learning based Optimization," *International Journal of Renewable Energy Research*, vol. 10, no. 1, pp. 366-377, 2020. [Google Scholar]